

# R-BENCH: ARE YOUR LARGE MULTIMODAL MODEL ROBUST TO REAL-WORLD CORRUPTIONS?

Chunyi Li<sup>1</sup>, Jianbo Zhang<sup>1</sup>, Zicheng Zhang<sup>1</sup>, Haoning Wu<sup>2</sup>, Yuan Tian<sup>1</sup>,  
Wei Sun<sup>1</sup>, Guo Lu<sup>1</sup>, Xiaohong Liu<sup>1</sup>, Xiongkuo Min<sup>1</sup>, Weisi Lin<sup>3</sup>, Guangtao Zhai<sup>1</sup>

<sup>1</sup>Shanghai Jiaotong University, <sup>2</sup>IN.AI, <sup>3</sup>Nanyang Technological University

<https://github.com/Q-Future/R-Bench>

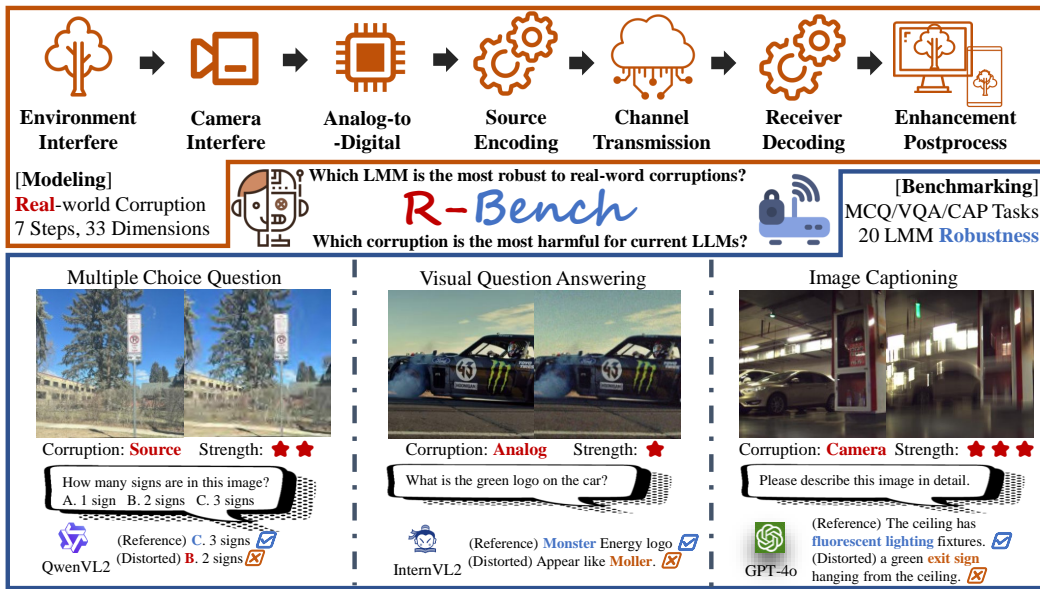


Figure 1: The construction overview of the proposed **R-Bench**. We model the full-link real-world corruption and evaluate the performance of LMMs on reference/distorted (left/right) images. Experiments demonstrate that the LMMs **solve the original image** but **hallucinate against corruption**.

## ABSTRACT

The outstanding performance of Large Multimodal Models (LMMs) has made them widely applied in vision-related tasks. However, various corruptions in the real world mean that images will not be as ideal as in simulations, presenting significant challenges for the practical application of LMMs. To address this issue, we introduce R-Bench, a benchmark focused on the **Real-world Robustness of LMMs**. Specifically, we: (a) model the complete link from user capture to LMMs reception, comprising 33 corruption dimensions, including 7 steps according to the corruption sequence, and 7 groups based on low-level attributes; (b) collect reference/distorted image dataset before/after corruption, including 2,970 question-answer pairs with human labeling; (c) propose comprehensive evaluation for absolute/relative robustness and benchmark 20 mainstream LMMs. Results show that while LMMs can correctly handle the original reference images, their performance is not stable when faced with distorted images, and there is a significant gap in robustness compared to the human visual system. We hope that R-Bench will inspire improving the robustness of LMMs, **extending them from experimental simulations to the real-world application**.

## 1 INTRODUCTION

Large Multimodal Models (LMMs) have demonstrated outstanding abilities in a wide range of visual tasks. Due to the cross-modal interaction capabilities brought by instruction tuning, they can

accurately understand visual information and provide precise feedback based on queries. However, unlike single-modal Large Language Models (LLMs), which have become the foundation of daily life for humans, satisfying diverse needs such as writing, searching, and coding, LLMs, despite their excellent performance, have not yet reached the same status. From the neural perception perspective (Zhang et al., 2022), the visual cortex accounts for at least 70% of the external information processing; and according to Cisco statistics (Cisco, 2020) from 2018-2023, image/video data accounted for 82% of network bandwidth. Therefore, if the real-world applications of LLMs can be expanded from text to images, it will bring tenfold convenience to daily human life.

**Why are LMMs excellent in benchmarks but limited in the real-world?** Robustness is a crucial factor. In experiments, LMMs usually receive high-quality images, but in real-world scenarios that includes numerous corruption, such as object motion, lens blur, etc. Worse still, in embodied AI or mobile devices (Bai et al., 2024) where agents call LMMs to perform tasks, due to the limitations of edge computing power, current models are mainly deployed on the cloud. The complex transmission process is also risky for corruption. Considering the image modality is much larger than text and encounters more losses in the real-world, LMMs must ensure robust results on distorted content.

Unfortunately, despite the emergence of benchmarks for LMMs in numerous tasks over the past few years, assessing their robustness in the real-world remains an unexplored challenge. First, the evaluation of robustness requires images before and after distortion, which presents a significant challenge in data collection. This involves modeling and categorizing corruptions on one hand, and maintaining carefully curated reference/distorted image pairs (rather than taking a bunch of distorted images directly) on the other. In addition, unlike the commonly used benchmark dimensions such as accuracy/recall, robustness currently lacks a universally accepted metric.

Considering these issues, we have established R-Bench to evaluate the robustness of LMMs in the real world. R-Bench aims to test the resistance of different LMMs to corruptions and to identify the most significant corruptions affecting LMMs' performance, thereby pointing out optimization directions for future LMMs and helping them adapt to real-world images, as shown in Figure 1. Our contributions can be summarized as follows:

- A comprehensive modeling of corruption to date. We have considered the entire link from image capturing to LMMs finally seeing the image based on knowledge in imaging science and communication engineering, and categorized it into 7 steps, and by underlying features into 7 groups, totaling 33 corruption dimensions in 3 different strengths.
- A large dataset containing 2,970 pairs of corresponding reference/distorted images, meticulously annotated by human experts, covering the three most mainstream tasks of LMMs. The data characteristics prove that they are suitable as a testing sequence for robustness.
- A comprehensive benchmark experiment that considers the performance of 20 mainstream LMMs on reference/distorted images, thereby measuring robustness. In particular, we have proposed the concepts of absolute/relative robustness with a mathematical definition, establishing a standardized process for future robustness evaluation.

## 2 RELATED WORKS

For the task of generating text from images, its robustness has been the long-term research topic as listed in Table 1. However, a series of works, including RobustBench, MSRVTT-P, AttackVLM, and OpenRedTeaming (Croce et al., 2021; Schiappa et al., 2022; Zhao et al., 2023; Cui et al., 2024), have treated robustness as a typical adversarial task. The distortions in images come from manual attacks, such as manually adjusting a part of the image or injecting carefully designed noise to induce the model to make mistakes. Although they study robustness, these distortions are completely different from the corruption in the real world. RobustVLM (Schlarmann & Hein, 2023) is the first study on corruption robustness, but its range of distortions is not rich enough. Subsequently, MMRobustness (Qiu et al., 2024) and MMC-Bench (Zhang et al., 2024a) considered more detailed distortion scenarios. However, their assessments of robustness are not reasonable enough; the former directly uses the task score of the distorted images as robustness, while the latter measures the similarity between the distorted images and the answers to the original images. Both of these evaluation mechanisms are irrational, which will be analyzed in Section 3.3.

Table 1: Comparision between previous robustness-related benchmark and R-Bench. R-Bench is more comprehensive and reliable in real-world evaluations.

Benchmark	Mechanism	Dimensions	Task	Robustness
RobustBench	Handcraft Attack	15	MCQ	Absolute
MSRVTT-P	Handcraft Attack	7	CAP	Absolute, Similarity
RobustVLM	Machine Corruption	2	CAP	Absolute, Similarity
AttackVLM	Generative Attack	2	CAP	Similarity
OpenRedTeaming	Handcraft Attack	3	MCQ, VQA, CAP	Absolute
MMRobustness	Machine Corruption	14	VQA, CAP	Absolute
MMC-Bench	Machine Corruption	29	CAP	Similarity
<b>R-Bench</b>	<b>In-the-wild, Machine Corruption</b>	<b>33</b>	<b>MCQ, VQA, CAP</b>	<b>Absolute, Relative</b>

In addition, all previous research on robustness has two common issues. First, very few works can simultaneously consider the three classic LMM tasks, namely Multiple Choice Questions (MCQ), Visual Question Answering (VQA), and Captioning (CAP). This limits the credibility of the benchmark in terms of robustness. Moreover, although some corruption comes from the real-world, they only include the machine transmission process from the captured image to LMM reception; they ignore the former process in obtaining the image itself, namely in-the-wild corruption. Therefore, an objective and reliable benchmark needs to be conducted to analyze robustness across multiple tasks and dimensions along the entire real-world corruption link.

### 3 BENCHMARK CONSTRUCTION

#### 3.1 REFERENCE DATA COLLECTION

To comprehensively characterize image data from the real world, we collect high-quality reference data and then add corruption to obtain distorted images. The selection of references is based on three principles: (1) Diversity: The data must contain different subjects, backgrounds, styles, etc., and the three tasks should be as evenly distributed as possible to avoid affecting the credibility of the benchmark due to highly consistent data. (2) Reality: The images must come from natural scenes, such as UGC (user-generated content) taken by average users. Content commonly found in other benchmarks, such as anime (Li et al., 2022), screen content (Li et al., 2024d), and AI-Generated Content (AIGC) (Li et al., 2024b;c; 2023) will be filtered out. (3) Quality: As high-quality reference information, the images must not already be distorted, as otherwise, they cannot be distinguished from the corresponding distorted images.

To obtain reference images, we have implemented the following mechanisms: First, we considered samples from today’s mainstream benchmarks, including seven LMM benchmark datasets for MCQ, VQA, and CAP tasks. (Lin et al., 2014; Liu et al., 2023c; Wu et al., 2023a; XAI, 2024; Liu et al., 2023a; Yu et al., 2024; Marino et al., 2019) Moreover, considering the needs of cloud-side LMMs in the embodied AI, we collected data by operating robots in various indoor, architectural, and street environments. Secondly, we recruited human experts to inspect the images and only retained those marked as in-the-wild. Finally, we used the most accurate Image Quality Assessment (IQA) models Q-Align, TOPIQ, and LIQE (Wu et al., 2023b; Chen et al., 2024a; Zhang et al., 2023) as quality controllers, representing the quality from semantic to pixel levels. If any of the indicators is below a certain threshold, the image is deemed to be distorted and removed. The specific image proportions and processing details are included in the Appendix. Finally, we add question-answer pairs to these images. For samples from other datasets that already included question-answer pairs, we retain them if our human experts could correctly answer. Otherwise, we re-annotate them. We also set new question-answer pairs for all samples we collected ourselves. As a result, we obtained 1,485 question-answer pairs, with 495 samples each for MCQ, VQA, and CAP as ground truth.

#### 3.2 DISTORTED DATA COLLECTION

To comprehensively characterize the corruption that images encounter in the real world, we divide the process from image capture to large model reception into seven steps: Environment Interference (EI), Camera Interference (CI), Analog-to-Digital (AD), Source Encoding (SE), Channel Transmis-

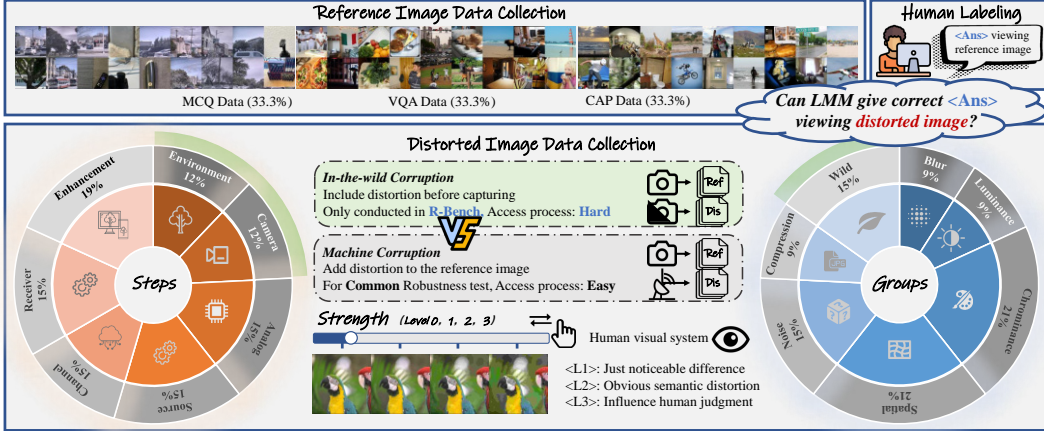


Figure 2: Data collection process of **R-Bench**. We collect and annotate reference image data with 3 different tasks, then construct distorted images with **In-the-wild corruption** by changing the environment before imaging, and **Machine corruption** by adding distortions. All 33 corruption dimensions belong to 7 **steps** (in time order) and 7 **groups** (in low-level), each having three levels of strength.

Table 2: All 33 corruption dimensions of R-Bench, listed by 7 distortion steps. Different icons denote 7 low-level group Blur (○), Luminance (□), Chrominance (△), Spatial (◊), Noise (★), Compression (+), and Wild (×).

Step	Explanation	Dimensions
Environment Interfere (EI,1)	Interference with the subject to be photographed	1.Motion blur ○; 2.Bright illumination ×; 3.Dark illumination ×; 4.Blocking obstacle ×
Camera Interfere (CI,2)	Interference with the photographing equipment	5.Lens blur ○; 6.Resolution limit ◊; 7.Lens obstacle ×; 8.Lens shaking ×
Analog-to-Digital (AD,3)	Analog-to-Digital conversion mistake by electronic devices	9.White Noise ★; 10.Color Noise ★; 11.Impulse Noise ★; 12.Multiplicative noise ★; 13.Clock jittering ◊
Source Encoding (SE,4)	Information discarded in the source encoding	14.Color quantization △; 15.JPEG2000 codec +; 16.JPEG codec +; 17.WEBP codec +; 18.Grayscale quantization ◊
Channel Transimssion (CT,5)	Information lost in channel transmission	19.Block exchange ○; 20.Block repeat ◊; 21.Block lost ◊; 22.Block interpolation ◊
Receiver Decoding (RD,6)	Information misinterpreted in the receiver decoding	23.HSV saturation △; 24.LAB saturation △; 25.Maximum brighten □; 26.Minimum darken □; 27.Mean shift □
Enhancement Postprocess (EP,7)	New corruptions introduced to recover above corruptions	28.Gaussian filter ○; 29.Color diffusion △; 30.Color shift △; 31.CNN denoise ★; 32.Shapness change △; 33.Contrast change △

sion (CT), Receiver Decoding (RD), and Enhancement Postprocess (EP). Unlike traditional robustness tests, we are the first to focus on the first two steps, EI and CI, which refer to the in-the-wild corruption encountered during the image capture process. We are not only concerned with the corruption that occurs after the image is captured, due to machine signal processing, transmission, and other issues. Note that in-the-wild corruption is more difficult to obtain than machine corruption. It requires changing environmental conditions and camera parameters in reality after capturing high-quality reference images, rather than applying perturbation strategies directly to the reference images as is done with the last five steps. Specifically, we considered 33 common corruption scenarios in the real world as dimensions for our benchmark. These dimensions can be divided into seven steps as mentioned; or, like past IQA work, they can also be categorized by low-level attributes into seven groups: Blur, Luminance, Chrominance, Spatial, Noise, Compression, and the in-the-wild corruption that R-Bench introduced for the first time. Table 2 shows the steps and groups to which each dimension belongs, as well as the definitions of each step. The definitions of each group are based on KADID-10K. (Lin et al., 2019) As space limits, the specific definitions of the 33 dimensions, as well as visual examples, are provided in the Appendix.

Note that we also controlled the intensity of corruption, which is beneficial for detecting the robustness of LMMs under different corruption levels, as shown in Figure 2. Based on the perceptual

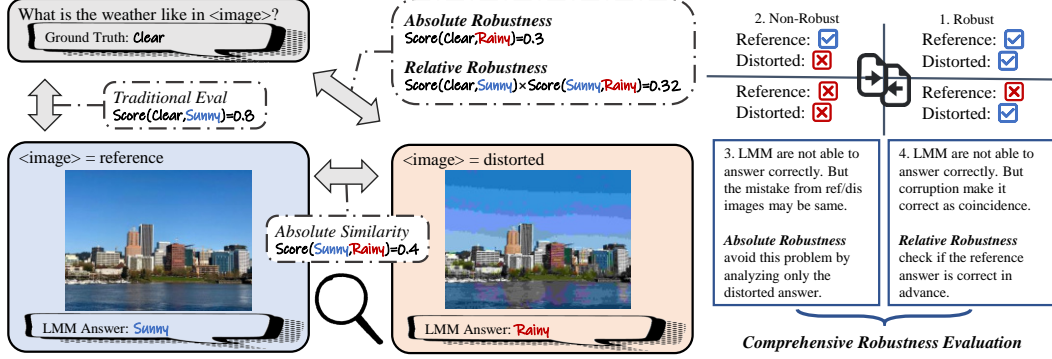


Figure 3: A comprehensive robustness evaluation example. The combination of absolute and relative robustness avoids misjudgment of chance examples, ensuring the reliability of the R-Bench.

mechanism of the HVS, the corruption is divided into three levels: low: humans can detect the difference between the distorted and reference images, which corresponds to the Just-Noticeable Difference (JND) in signal processing; mid: there is a noticeable semantic difference between the two images, but it does not affect human cognition; High: the corruption is severe enough to mislead humans, such as giving incorrect answers to questions like the number of people or the background objects in the image. Within R-Bench, we strictly controlled the intensity of the corruption when capturing distorted images and manually adding distortion, ensuring an average distribution of low/mid/high samples.

### 3.3 ROBUSTNESS DEFINITION

This section defines robustness mathematically to enable a comprehensive robustness assessment. Robustness can be categorized into absolute and relative aspects. Absolute robustness refers to the performance that LMMs exhibit only on distorted images, while relative robustness is whether the outputs of LMMs are stable between reference/distorted images. Thus, absolute robustness  $R_a$  can be simply defined as:

$$R_a = \text{Score}(GT, \text{LMM}(I_{dis})), \quad (1)$$

where function  $\text{Score}(\cdot)$  compute the similarity between ground truth answer  $GT$  and the LMM( $\cdot$ ) result when viewing the distorted image  $I_{dis}$ . However, this metric is not comprehensive; for a powerful LMM, its performance on distorted images may significantly decline compared to reference images, but since the baseline of the reference is already high, this does not necessarily lower the appearance of  $R_a$ . Thus, it can be termed a powerful model but not robust. Therefore, it is necessary to add a relative concept above absolute robustness. Some robustness studies (Zhao et al., 2023; Zhang et al., 2024a) attempt to directly express robustness through the output discrepancy between reference and distorted images. Unfortunately, this evaluation is even more unreasonable and can only be referred to as similarity, rather than robustness. For instance, if an LMM produces incorrect outputs, regardless of viewing the reference or distorted image, if these errors happen to be consistent, then this poor model will receive a perfect similarity score. Thus, we have initially defined relative robustness  $R_r$  as follows: **Provided that an LMM can correctly process reference images, if the distorted output is still consistent with the reference**, namely:

$$R_r = \text{Score}(GT, \text{LMM}(I_{ref})) \cdot \text{Score}(\text{LMM}(I_{ref}), \text{LMM}(I_{dis})), \quad (2)$$

where  $I_{ref}$  denotes the reference image. R-Bench will calculate the performance of all LMMs individually based on the above two metrics and use the average value for the final robustness ranking.

## 4 EXPERIMENT

### 4.1 BENCHMARK CANDIDATES

R-Bench uses 20 mainstream LMMs for testing. All chosen models have demonstrated excellent performance in past multi-modality understanding benchmarks (Liu et al., 2023c; Wu et al., 2023a;

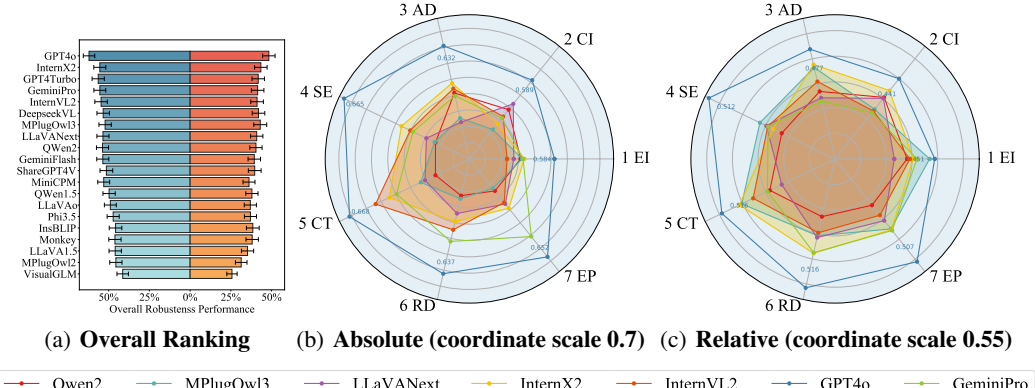


Figure 4: Result of R-Bench. (Zoom in to see details) **Absolute** robustness is demonstrated on the left side of (a) and (b); **Relative** robustness is demonstrated on the right side of (a) and (c). Overall the robustness of all LMMs is unsatisfactory, with the proprietary LMMs performing relatively stronger than the open-source. For corruption, Step 1: Environmental Interference and Step 2: Camera Interference has severe negative impacts on all LMMs.

Zhang et al., 2024b) that have relatively strong processing capabilities for reference images, thus ensuring that the robustness results derived by R-Bench are meaningful, including proprietary LMMs: GeminiFlash, GeminiPro (Team, 2024), GPT4o, GPT4Turbo (Achiam et al., 2023); and open-source as 7B-size: DeepseekVL (Lu et al., 2024), InstructBLIP (Dai et al., 2023), InternVL2 (Chen et al., 2024b), InternLM-XComposer2 (Dong et al., 2024), LLaVA1.5 (Liu et al., 2023b), LLaVANext (Li et al., 2024e), LLaVA-OneVision (Li et al., 2024a), MiniCPM (Yao et al., 2024), Monkey (Li et al., 2024f), MPlugOwl2 (Ye et al., 2024b), MPlugOwl3 (Ye et al., 2024a), Phi3.5 (Abdin et al., 2024), QWen1.5-VL (Bai et al., 2023), Qwen2-VL (Wang et al., 2024), ShareGPT4V (Chen et al., 2023), VisualGLM (Du et al., 2022). All LMMs are tested as zero-shot.

Regarding human robustness in the real-world, we conducted a user study in a controlled laboratory environment with five average subjects. They would first view examples of distortions across 33 dimensions and fully confirm that they could understand distorted images. Participants who did not meet the criteria would be excluded. Subsequently, they would watch images from the R-bench in a random order and provide appropriate answers to the questions. Note that for both the LMMs experiment mentioned above and the human subjects here, the MCQ/VQA/CAP tasks were interspersed to prevent any prior knowledge from making the participants familiar with a particular task, thus leading to artificially inflated performance. To avoid the strong resilience to distortions by a few people familiar with photography/communications, the averaged performance of participants except maximum and minimum will serve as the human baseline.

## 4.2 EVALUATION CRITERIA

In the MCQ, VQA, and CAP tasks, we use three LMM-assisted mechanisms as the Score function in Section 3.3. For MCQ, since most LMMs cannot consistently provide instructed output formats, we adopt the following method. If the LMM directly provides options in the form of 'A,B', we directly check the correctness of options; otherwise, we refer to the GPT evaluation proven effective by Liu et al. (2023c) to judge whether the output is semantically consistent with the ground truth. For VQA and CAP tasks, since traditional language metrics like BLEU, CIDEr, and SPICE (Papineni et al., 2002; Vedantam et al., 2015; Anderson et al., 2016) tend to penalize errors rather than reward correct answers, this can lead to advanced LMMs with more complete answers receiving lower scores. (Especially for relative robustness) Therefore, we adopt a similar approach to Q-Bench and A-Bench (Wu et al., 2023a; Zhang et al., 2024b), where a comprehensive score is given to the image based on completeness, precision, and relevance. For VQA, where the target output is less than 10 words, it can be directly compared to the ground truth; for CAP, where the output is around 40 words, we calculate the degree to which each score point in the GT is matched. We repeat the evaluation for each sample five times to avoid chance and collect the weighted average as the final score from 0 to 1. (The MCQ score is binaryized as correct or incorrect.)

Table 3: Results of Absolute (above) and Relative (below) robustness on MCQ/VQA/CAP tasks with 3 corruption strength levels, considering 16 open-source and 4 proprietary LMMs as underlined. The best/second results are marked in **Orange/Blue** respectively. Long-named models are abbreviated.

Absolute	MCQ			VQA			CAP			Overall	
	Strength	low	mid	high	low	mid	high	low	mid	high	
<u>GPT4o</u>		<b>0.8176</b>	<b>0.7744</b>	<b>0.7391</b>	<b>0.7184</b>	<b>0.7291</b>	<b>0.6898</b>	<b>0.4235</b>	<b>0.4200</b>	<b>0.3997</b>	<b>0.6348</b>
<u>GPT4Turbo</u>		0.7059	0.6398	0.6220	<b>0.7055</b>	<b>0.7048</b>	<b>0.6806</b>	0.3698	0.3811	0.3383	<b>0.5722</b>
<u>GeminiPro</u>		<b>0.7529</b>	0.7012	0.6708	0.6233	0.6315	0.5796	0.4006	<b>0.4040</b>	0.3734	0.5710
InternX2		0.7176	0.6770	0.6220	0.6288	0.6255	0.6180	0.4204	0.3982	0.3659	0.5638
InternVL2		0.7118	<b>0.7019</b>	0.6280	0.6442	0.6436	0.6383	0.3759	0.3669	0.3412	0.5614
<u>GeminiFlash</u>		0.7235	0.6708	<b>0.7073</b>	0.5975	0.6036	0.5575	0.3840	0.3522	0.3487	0.5495
LLaVANext		0.6529	0.6087	0.5732	0.6276	0.6382	0.6150	0.3957	0.4006	0.3873	0.5445
MiniCPM		0.7081	0.6471	0.5610	0.5626	0.6024	0.5880	0.4025	0.4047	<b>0.3885</b>	0.5405
Qwen2-VL		<b>0.6765</b>	0.6708	0.5732	0.5914	0.6024	0.5335	0.4142	0.4127	0.3787	0.5393
DeepseekVL		0.6149	0.5824	0.5244	0.6679	0.6227	0.6383	0.4167	0.4043	0.3741	0.5384
MPlugOwl3		0.6706	0.6398	0.6159	0.5920	0.5715	0.5671	0.3728	0.3729	0.3729	0.5307
ShareGPT4V		0.6273	0.5588	0.5488	0.6227	0.6145	0.6473	0.3716	0.3769	0.3390	0.5229
Qwen1.5-VL		0.6087	0.5765	0.5000	0.6178	0.5642	0.5964	0.3895	0.3717	0.3502	0.5083
LLaVAo		0.5353	0.5652	0.5305	0.5387	0.5255	0.5749	<b>0.4259</b>	0.3990	0.3809	0.4972
Phi3.5		0.5765	0.5652	0.5244	0.5337	0.5679	0.5114	0.3660	0.3564	0.3342	0.4818
Monkey		0.5471	0.5155	0.4451	0.5712	0.5648	0.5413	0.3833	0.3487	0.3573	0.4750
LLaVA1.5		0.4706	0.4596	0.4695	0.6049	0.5679	0.6210	0.3457	0.3433	0.3476	0.4701
MPlugOwl2		0.5647	0.5652	0.5000	0.5245	0.5255	0.5311	0.3364	0.3284	0.3043	0.4645
InstructBLIP		0.4529	0.5280	0.4756	0.5534	0.5467	0.5653	0.3284	0.3414	0.3557	0.4606
VisualGLM		0.4765	0.5217	0.5061	0.3994	0.3885	0.3623	0.3864	0.3571	0.3830	0.4198
Relative	MCQ			VQA			CAP			Overall	
Strength	low	mid	high	low	mid	high	low	mid	high		
<u>GPT4o</u>		<b>0.7471</b>	<b>0.6894</b>	<b>0.6159</b>	<b>0.5787</b>	<b>0.5725</b>	<b>0.5622</b>	0.2274	0.2134	0.2083	<b>0.4907</b>
InternX2		0.6353	0.6087	0.5488	0.5038	0.5127	0.4639	0.2440	0.2317	0.2070	<b>0.4396</b>
MPlugOwl3		0.6087	0.5882	0.5488	0.5242	0.4877	0.4938	0.2423	0.2106	<b>0.2205</b>	0.4359
<u>GPT4Turbo</u>		0.5941	0.5590	0.4817	<b>0.5872</b>	<b>0.5575</b>	0.5196	0.1972	0.1910	0.1836	0.4302
DeepseekVL		0.5706	0.5342	0.4756	0.5384	0.5164	0.4934	<b>0.2540</b>	<b>0.2341</b>	0.2089	0.4251
<u>GeminiPro</u>		0.6706	0.6211	0.5793	0.4640	0.4799	0.4510	0.1773	0.1874	0.1649	0.4219
InternVL2		0.6294	0.6149	0.5427	0.4849	0.4850	0.4556	0.1940	0.1893	0.1698	0.4185
LLaVANext		0.5882	0.5155	0.4817	0.5061	0.5065	0.4531	0.2310	0.2159	0.2161	0.4129
Qwen2-VL		<b>0.6706</b>	<b>0.6522</b>	0.5244	0.4217	0.3926	0.3627	0.2210	0.2025	0.1957	0.4049
<u>GeminiFlash</u>		0.6235	0.5714	<b>0.6037</b>	0.4397	0.4719	0.4031	0.1681	0.1709	0.1654	0.4021
ShareGPT4V		0.5528	0.4941	0.4573	0.5067	0.4897	<b>0.5303</b>	0.2109	0.2032	0.1733	0.4019
Monkey		0.4647	0.4534	0.3598	0.5036	0.4882	0.4546	<b>0.2828</b>	<b>0.2451</b>	<b>0.2379</b>	0.3877
Qwen1.5-VL		0.5342	0.4941	0.4085	0.4712	0.4311	0.4637	0.2530	0.2152	0.2046	0.3860
InstructBLIP		0.4529	0.4720	0.4451	0.4937	0.4615	0.4738	0.2343	0.2302	0.2061	0.3855
LLaVAo		0.5059	0.5093	0.4817	0.4482	0.4224	0.4214	0.2078	0.2075	0.2012	0.3784
Phi3.5		0.5176	0.4845	0.4695	0.4564	0.4891	0.3896	0.1915	0.1950	0.1825	0.3751
MiniCPM		0.5176	0.5280	0.4512	0.3909	0.4233	0.4223	0.1967	0.1885	0.1955	0.3683
LLaVA1.5		0.4412	0.3727	0.3720	0.5101	0.4558	0.5101	0.1955	0.1883	0.1850	0.3592
MPlugOwl2		0.4529	0.4472	0.4146	0.3480	0.3659	0.3551	0.1676	0.1628	0.1507	0.3184
VisualGLM		0.3765	0.4161	0.3841	0.2038	0.1990	0.1722	0.1951	0.1911	0.2071	0.2604

#### 4.3 BENCHMARK RESULT AND DISCUSSION

Figure 4 shows the absolute and relative robustness of 20 LMMs. The 90% confidence intervals of each LMM are marked as error bars, indicating that the scores of the same LMM on different test samples are similar, indirectly proving that the results of the R-Bench test are stable and credi-

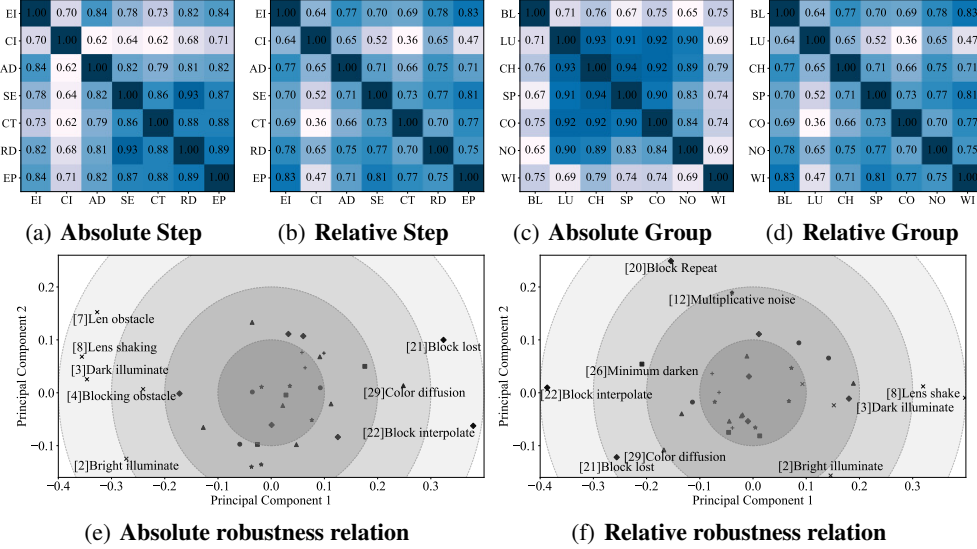


Figure 5: Correlation mat between 7 steps and 7 groups in absolute and relative quality. Principal components of all 33 corruption dimensions are analyzed. Prominent similarity is reflected by higher values from (a) to (d), and closer distance in (e) and (f). The shape of each point obeys Table 2.

ble. Figures (b) and (c) demonstrate that GPT4o is fully superior to other models in each distortion step, with an overwhelming advantage in absolute robustness and a slight lead in relative robustness. The open-source LMMs InternLM-XComposer2 and InternVL2 perform relatively well and can surpass proprietary LMMs (except GPT4o) in some dimensions. Most LMMs score lower in the first two steps, and relatively higher in the last five. This reflects that their training process may have incorporated machine-related distorted images, especially compressed and partially masked ones (which correspond to steps 4 and 5, where LMMs are currently most proficient), thus having some robustness. However, the wild-in-the-distortion data for the first two dimensions needs to be collected manually rather than relying on machine simulation, so LMMs find it difficult to handle this unseen corruption. Table 3 provides a detailed overview of the performance of LMMs under different tasks and corruption levels. Overall, closed-source models dominated the top three positions in terms of absolute robustness, while open-source models exhibited better relative robustness. In terms of tasks, the proficiency order of all LMMs is MCQ>VQA>CAP, indicating that as the output format becomes more complex, corruption becomes more likely to lead to incorrect outputs, which negatively impacts robustness; in terms of corruption level, the higher the level, the worse the LMM’s performance. This suggests that LMMs and humans generally share the same preference for distorted images, with only two exceptions. Firstly, some LMMs are most sensitive to the low>mid change, such as GPT4Turbo, yet are unaffected by mid>high corruption; some LMMs exhibit completely opposite sensitivities between the two, like Qwen2-VL. This suggests the ‘image quality degradation’ perceived by LMMs is not entirely linear. Secondly, we have found in a few cases that LMMs experience an increase in performance after corruption intensifies, such as ShareGPT4V in the VQA task. This indicates that corruption is not always detrimental, and specific corruptions may promote feature extraction in certain models, thereby stimulating the model emergence. (Wei et al., 2022) Both of these interesting findings warrant further investigation.

#### 4.4 CORRUPTION ANALYSIS

To explore the relationships between each corruption dimension, we calculated the SRoCC (Spearman Rank-order Correlation Coefficient) for the 7 steps and 7 groups of corruption, based on the performance of LMMs, as shown in Figure 5. The data from (a) to (d) show that the differences in relative robustness between models are greater than those in absolute robustness, with the results of steps such as Camera interfere and categories like Wild differing the most from the others. These dimensions include a large number of in-the-wild corruptions, and this difference also proves the necessity of considering corruption for the first time in the robustness evaluation. (e) and (f) take the performance of the 33 corruptions for a principal component analysis, with most objects distributed

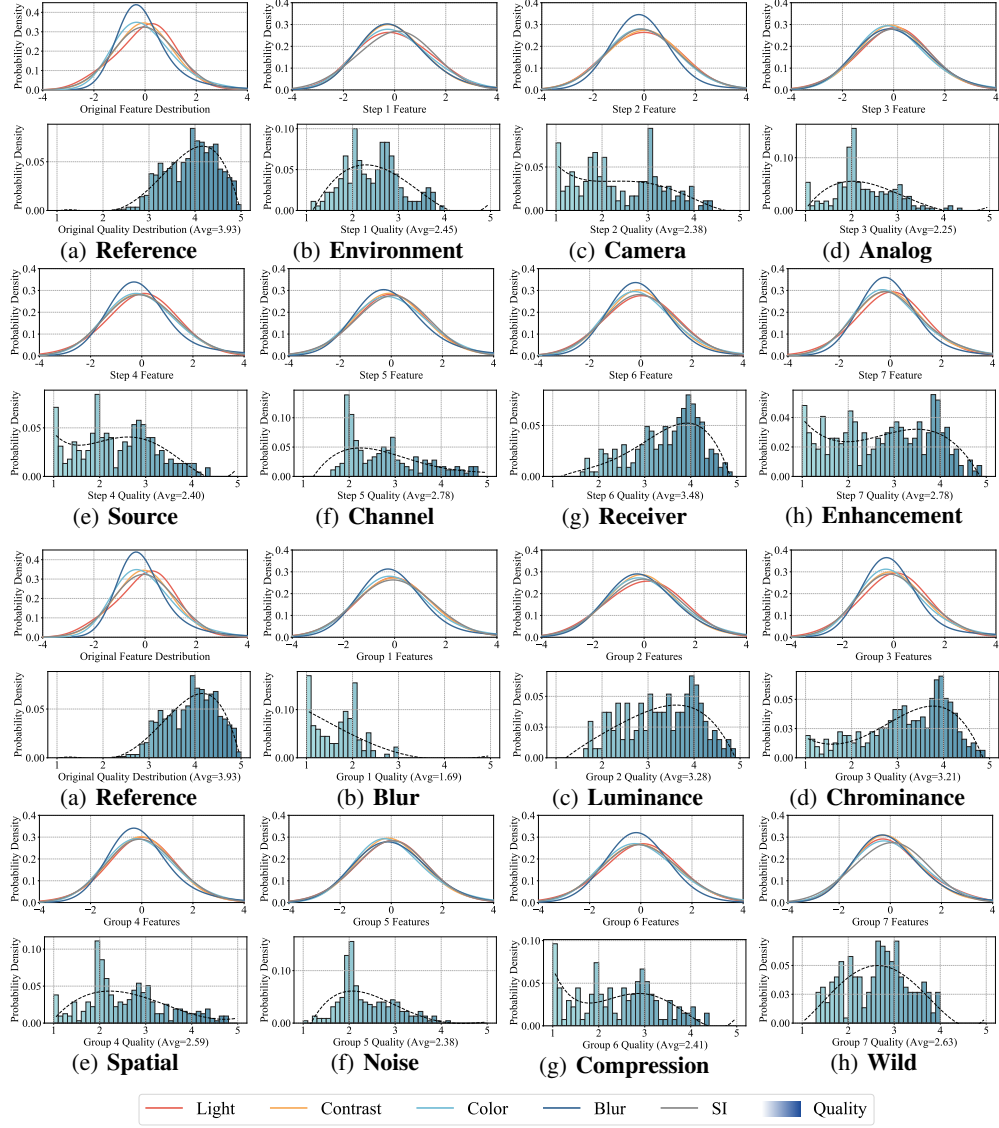


Figure 6: Low-level feature curve and quality distribution of reference/distorted images in different corruption steps/groups. Flatter curves and lower quality are more sensitive to corruption.

relatively close together, and sub-dimensions 2, 3, 8, 21, and 22 differing significantly from the others. Therefore, future robust LMMs need to focus on these aspects.

Figure 6 further analyzes the low-level features of the reference/distorted image in R-Bench. We calculated the distribution of five quality-related attributes, including light, contrast, color, blur, and Spatial Information (SI, representing the content diversity of the image). Detailed explanations of these attributes can be found in work (Hosu et al., 2017). Specifically, the flatter the distribution, the more extreme values are represented, implying such corruption changes the image more. Meanwhile, we calculate the low-level quality distribution for each corruption step and group using Q-Align, (Wu et al., 2023b) and label the mean value on the x-axis. Considering the above two factors together, we find the steps EI/AD/CT, and group Blur/Noise bring the most significant corruption to the image. However, the dimensions that hallucinate LMMs most in Figures 4 and 5, Step: CI, and Group: Wild do not change significantly. Summarizing the above information, we conclude that the results for the perception of image corruption were different at the signal processing level, human subjective level, and the LMM level. Therefore, the perceptual mechanism of LMM will be the key to solving its real-world robustness problem.

Table 4: Absolute robustness comparison between *GPT-4o* and *human (left/right)*. Evaluated by 3 tasks, 3 strength, 7 steps, and 7 groups. As the R-bench champion, *GPT-4o* still lags behind *human* across the board. **Orange/Blue** denote *GPT-4o* performance below 90% or above 98% of *humans*.

Task	MCQ	VQA	CAP	Strength	low	mid	high
	0.735/0.909	0.712/0.678	0.414/0.425		0.644/0.671	0.615/0.670	0.604/0.672
Step	Environment	Camera	Analog	Source	Channel	Receiver	Enhancement
	0.578/0.625	0.572/0.602	0.614/0.675	0.656/0.663	0.657/0.713	0.620/0.708	0.634/0.692
Group	Blur	Luminance	Color	Spatial	Noise	Compress	Wild
	0.604/0.622	0.621/0.684	0.647/0.693	0.651/0.686	0.613/0.675	0.666/0.684	0.533/0.629

#### 4.5 GPT4O VS HUMAN

Given that the robustness of GPT leads in various downstream tasks, corruption intensity, and across the majority of dimensions compared to all existing LMMs, we compare it with human performance in Table 4. Since answers from humans on reference images are almost GT, there is no statistical difference in absolute/relative robustness. Therefore, we only compare absolute robustness, which is where LMMs are more proficient. Unfortunately, we find that GPT4o still has a significant gap compared to humans, although it achieved a perfect score in the R-Bench evaluation. The only task where GPT4o surpasses human performance is VQA, and the main reason is the openness of the questions, leading to different answers from humans for the same sample, rather than corruption’s influence. In addition, only Step: SI reaches 98% of human performance. In other aspects, GPT4o shows a comprehensive disadvantage, especially in MCQ tasks and at high corruption levels; in addition, Steps: RD and Group: Wild are the main sources of the gap.

In summary, based on the above analyses, we believe that current LMMs have some robustness against corruption but are not suitable for the real world. To address the variety and severity of corruption in the real world, further optimization is needed in the following aspects:

- For LMMs: The optimization focus for proprietary LMMs is on relative robustness, ensuring that the output on distorted images matches that of reference images, gradually approaching and potentially surpassing human performance. Open-source LMMs, however, first need to ensure absolute robustness, achieving correct results on reference images, and improving their resilience to corruption only after enhancing their original performance.
- For corruption: In the link from the agent capturing to the LMM perceiving, the first two steps, which are in-the-wild distortions, need to be given special attention. Their negative impact on model robustness far exceeds that of the subsequent five steps related to machines. On the one hand, LMM developers need to use more distorted data for training; on the other hand, current users need to avoid such issues when using LMMs.
- For robustness itself: Assessing LMM robustness is currently the biggest challenge. Experiments show that in some dimensions, there is a significant decline in image quality, yet the performance of LMMs is barely affected; while in other relatively minor distortions, LMMs produce severe hallucinations. In the future, an end-to-end assessment for LMM robustness is needed, explaining the correlation between corruption and LMM perception mechanisms, thereby inspiring LMMs to handle various images in the real world.

## 5 CONCLUSION

We construct R-Bench, a benchmark for evaluating the robustness of LMMs in the real world against corruption, indicated by the performance of LMMs on distorted images in three downstream tasks: MCQ, VQA, and CAP. We fully modeled the pipeline from the agent capturing to the LMM perceiving for the first time, and classified 33 common corruptions in the real world, including 7 time steps and 7 low-level groups with high-quality human annotations. Through our first-ever absolute-relative comprehensive robustness evaluation, we find that proprietary models outperform open-source models but still significantly lag behind humans, which are not yet ready for the real-world. Extensive experimental analysis of corruption also reveals factors that lead to the lack of robustness. We sincerely hope that R-Bench will inspire future LMMs to achieve better robustness, extending their applications from experimental simulations to the real-world.

## A APPENDIX

### A.1 LIMITATIONS AND SOCIAL IMPACT

**Limitation 1:** Although R-Bench considers a wide range of LMMs, there are always more advanced models that cannot be taken into account. Especially for the robustness task, experiments have shown that LMMs do not lack the relevant knowledge, but are guided to hallucinate by corruption, thus giving incorrect answers. With the rapid iteration of LMMs, although we regret that we cannot test these upcoming advanced models, we sincerely hope that the current R-Bench can be an assistant for future LMM evolution on robustness.

**Limitation 2:** Although the evaluation of R-Bench is comprehensive and reliable, it still needs assistance from text-modal GPT, which is a common problem of many current benchmarks. (Wu et al., 2023a; Zhang et al., 2024b; Liu et al., 2023c) This limits its usage as a reference list for the model level, rather than an evaluation plug-in for the instance level. For the evolution of LMM, if the image preference of LMM can be obtained in real-time through an open-source pipeline, robustness can be measured through Reference/Distorted image score disparity. This will be very helpful for its understanding and processing of distorted images, thus improving its usability in the real-world.

**Social Impact:** We believe R-Bench can drive innovation by providing a standardized platform for comparing different models and their resilience against corruption. Evaluating how well LMMs handle imperfections can significantly enhance the reliability of real-world downstream tasks, helping them meet certain robustness standards before deployment. This is crucial for applications where accuracy is critical while corruption is easy to occur, such as medical imaging, autonomous vehicles, and embodied AI.

### A.2 CORRUPTION DETAIL

All 33 corruption are listed below, with the (Step, Group) they belong to:

1. Motion blur (EI, Blur): The object itself is moving, causing a blur trail.
2. Bright illumination (EI, Wild): A very bright light source in the environment, interfering with the imaging.
3. Dark illumination (EI, Wild): No light source in the environment, making it difficult to image.
4. Blocking obstacle (EI, Wild): An obstacle blocks part of the object being photographed.
5. Lens blur (CI, Blur): Lens fog causes refraction.
6. Resolution limit (CI, Spatial): The lens resolution is insufficient, requiring upsampling.
7. Lens obstacle (CI, Wild): An obstacle blocks part of the lens.
8. Lens shaking (CI, Wild): The camera shakes randomly in the direction of movement, making it difficult to capture clear images.
9. White Noise (AD, Noise): Overall aging or prolonged operation of the circuit causes noise.
10. Color Noise (AD, Noise): Damage to certain channels in the YCbCr of the circuit components.
11. Impulse noise (AD, Noise): External factors cause sudden interference to the circuit components.
12. Multiplicative noise (AD, Noise): The power supply voltage does not match the required voltage of the circuit components.
13. Clock jittering (AD, Spatial): The frequency of the clock module is inaccurate, causing frequency oscillation.
14. Color quantization (SE, Chrominance): Similar colors are merged through minimum variance quantization.
15. JPEG2000 codec (SE, Compression): A standard image compression method.
16. JPEG codec (SE, Compression): The most widely used image compression method.
17. WEBP codec (SE, Compression): The image compression method with the best comprehensive performance.
18. Grayscale quantization (SE, Spatial): 256 colors are mapped to fewer dimensions through uniform quantization.
19. Block exchange (CT, Spatial): The order of two Macro-blocks in the channel is wrong.
20. Block repeat (CT, Spatial): A Macro-block is convoluted twice and covers the original position.
21. Block lost (CT, Spatial): A Macro-block is lost, and some communication protocol turns it into random pixels.

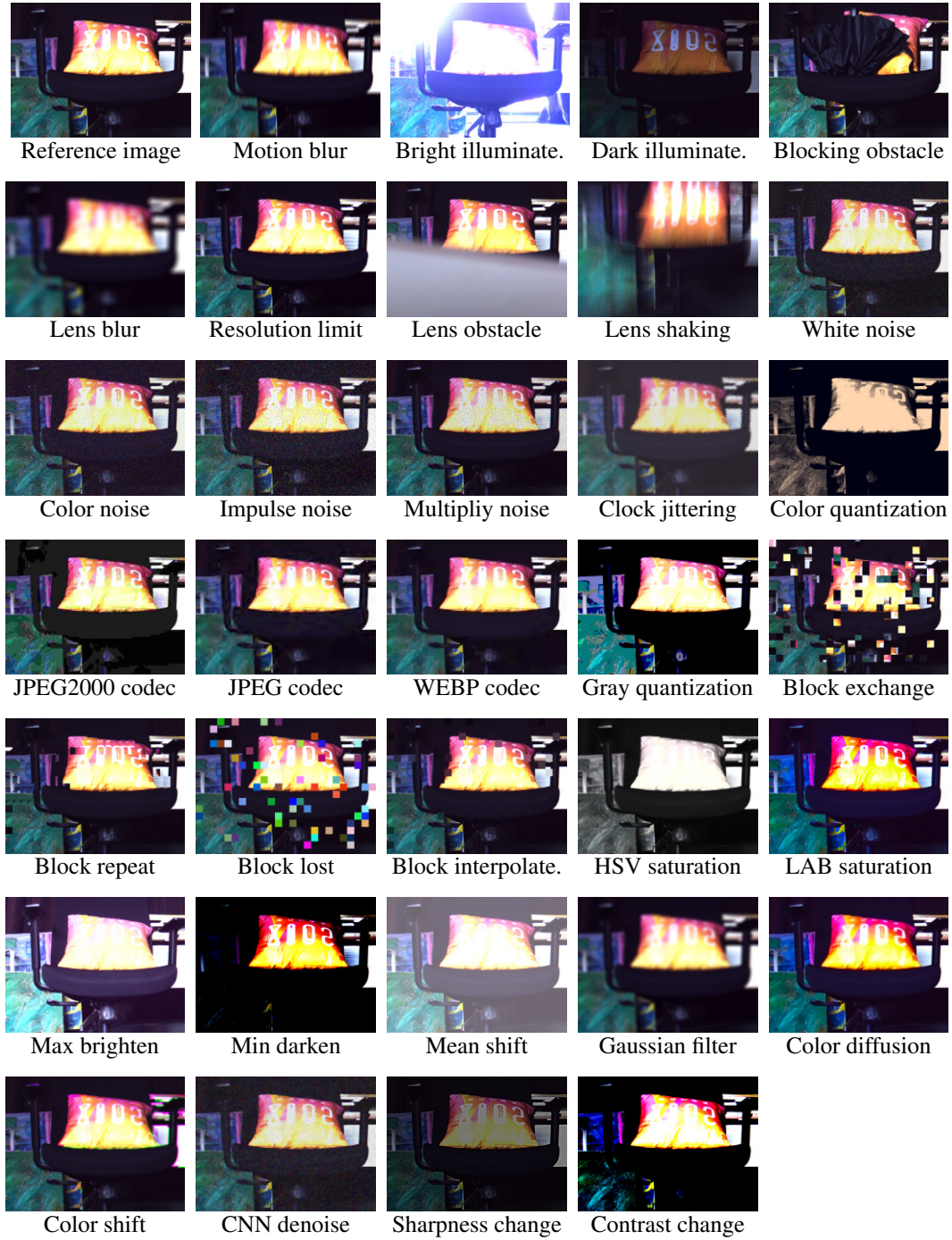


Figure 7: Visualization example of the reference image and its all 33 corruption example. Corruption names will be abbreviated if too long.

22. Block interpolation (CT, Spatial): A Macro-block is lost, and some communication protocol uses surrounding pixels to interpolate it.
23. HSV saturation (RD, Chrominance): The saturation channel of the HSV image is incompatible with the decoder.
24. Lab saturation (RD, Chrominance): The color channel of the Lab image is incompatible with the decoder.

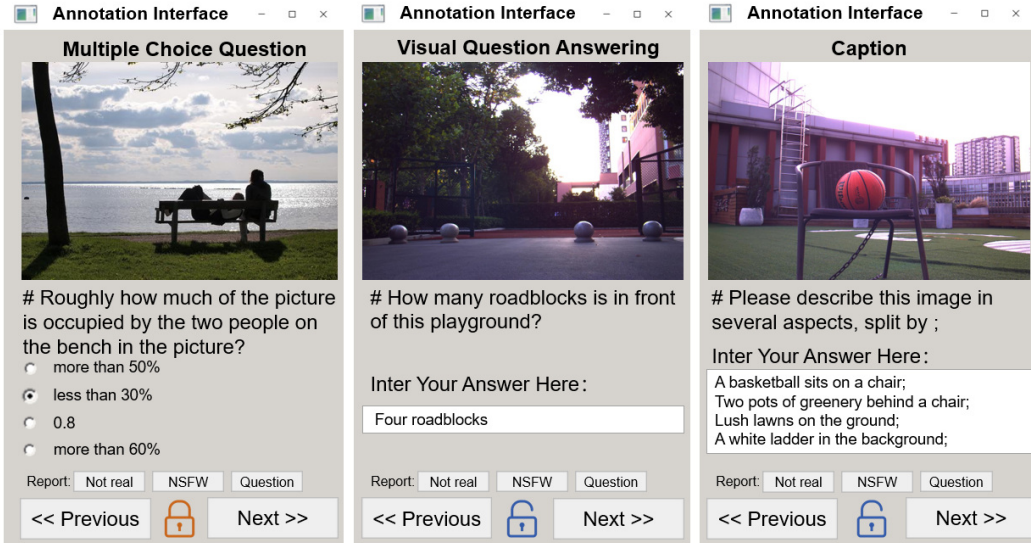


Figure 8: Human user interface for labeling. Three tasks will come in random order.

25. Maximum brighten (RD, Luminance): Some non-linear decoders keep the maximum value unchanged and increase other pixel values.
26. Minimum darken (RD, Luminance): Some non-linear decoders keep the minimum value unchanged and decrease other pixel values.
27. Mean shift (RD, Luminance): Some decoders automatically adjust contrast, but sudden changes in lighting are not yet adapted.
28. Gaussian filter (EP, Blur): New noise introduced by removing grainy salt-and-pepper noise.
29. Color diffusion (EP, Chrominance): New noise introduced by removing certain salt-and-pepper noise in one channel.
30. Color shift (EP, Chrominance): Unreasonableness introduced through the recovery of another missing channel through a certain channel.
31. CNN denoise (EP, Noise): AI-artifacts introduced through neural networks in image-reconstruction or super-resolution tasks.
32. Sharpness change (EP, Chrominance): Over-sharpening caused by excessive configuration of the sharpness by some users.
33. Contrast change (EP, Chrominance): Details lost due to excessive configuration of the contrast by some users.

The example of all corruption is shown in Figure 7, for clear visualization, the corruption strength is set as ‘high’. Overall, the content of each Step and Group is relatively homogeneous, with none of them containing too many or too few sub-dimensions, justifying the categorization.

### A.3 USER INTERFACE

The user annotation interface is shown by Figure 8, where subjects will complete interspersed MC-Q/VQA/CAP tasks in a randomized order, with some samples being annotated and others not. Subjects can make the following decisions:

- If they agree with the labeling, then click Next;
- If they do not agree with the annotation, they click Unlock to get permission to re-edit the content;
- If the question itself does not make sense, click Question in Report, and the image will be sent to the R-Bench expert team to redesign the question;
- If seeing an unnatural image, or NSFW content is found, click the corresponding button in Report, and this sample is excluded from R-Bench.

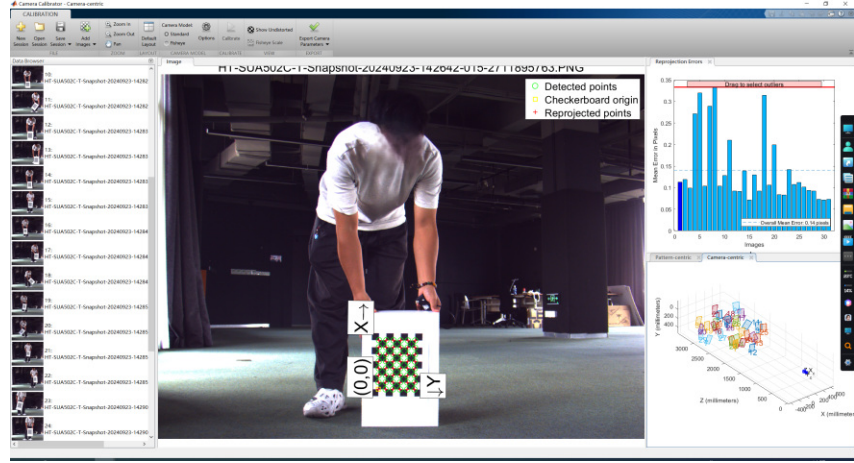


Figure 9: Camera parameter labeling with the mosaic board. The expert face is masked for privacy.

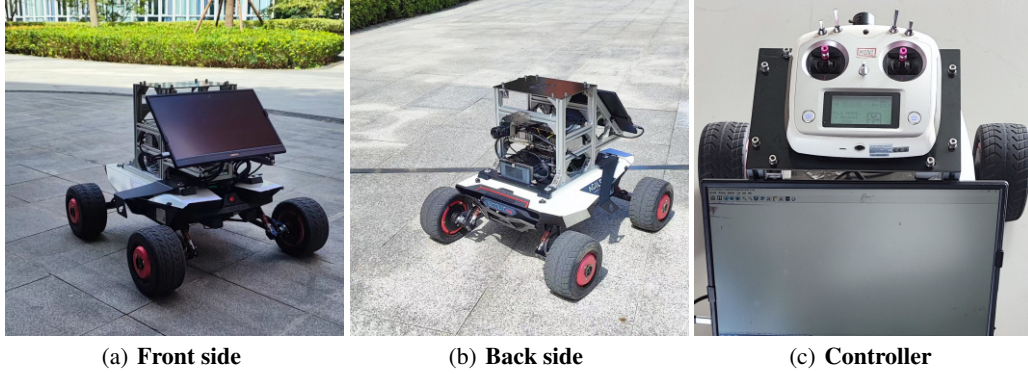


Figure 10: The final assembled robot.

The word limits for VQA and CAP tasks are 10 and 40, and we do not encourage users to write too long content. All labeled content will be reviewed by the R-Bench team to eliminate low-quality data and reserve high-quality data from 5 subjects, thus ensuring the reliability of the benchmark.

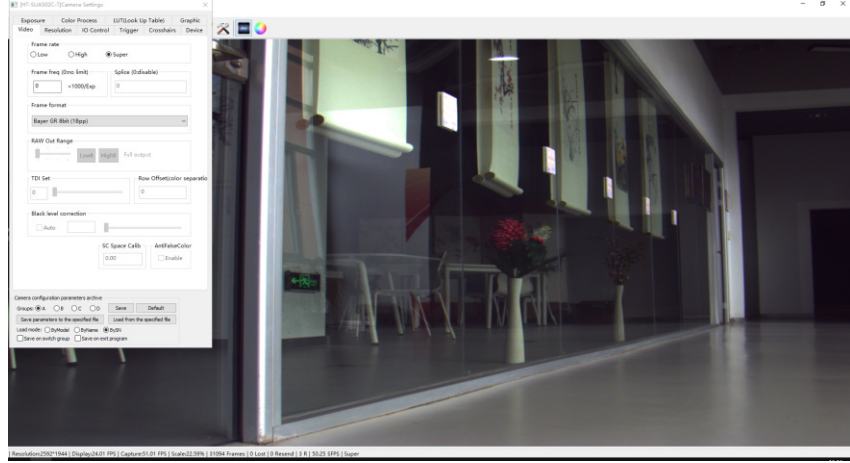
#### A.4 IMAGE COLLECTION PROCESS

The R-Bench author team has a rich cross-disciplinary background, including computational photography, bit-attitude estimation, robot manipulation, source/channel coding, and many other techniques. Together, they ensured a smooth implementation of R-Bench. The data outside of the in-the-wild in the 33 corruption dimensions was handled by the channel group. They are responsible for manually collecting the data and simulating the distortion using Matlab. The more difficult in-the-wild data is taken care of by the robotics group, i.e., the reference/distortion images are collected in the same scene. Therefore, the robotics group needs to make sure that both the first image taken is of high quality, and the second image needs to be identical to the first one in terms of scenery except for the target distortion. In order to shorten this interval, the camera needs to be fully set up in advance.

We first assembled the camera with the robot. The camera is HUATENGVISION HT-SUA502C and the robot is Agilex Scout Mini. At this point, due to some deviation in the camera position, a correction is required to ensure the quality of the reference image.

Then, the camera calibration is performed, we use the classic mosaic calibration plate to calculate the degree of offset of the bit position, from which the initial parameters of the camera are adjusted, as shown in Fig. 9. The result is listed as:

$$\text{Focal Length}(fx, fy) = [3460.8, 3391.3]$$



(a) Robot see before distortion



(b) Actual lens obstacle (c) Actual lens obstacle (d) Actual lens shaking (e) Actual lens shaking

Figure 11: Robot before encountering corruptions.

$$\text{Principal Point}(cx, cy) = [1270.9, 990.06]$$

$$\text{Radial Distortion} = [-0.1235, 0.2016]$$

The final assembly is shown in Fig. 10. Next, we manipulate the robot to collect samples in a variety of environments, including indoors, in the field, in buildings, on streets, and in garages. We will first take a high-quality image and then immediately manipulate the robot to introduce corruption and take a second distorted image. Figure 11 illustrates this process completely taking dimension 7 lens obstacle and 8 lens shaking as examples. Finally, R-Bench’s team of experts will review the two images to see if the difference is large enough and exclude it if it is not significant.

In summary, it can be seen that reference/distorted image pairs are much more difficult to acquire in the in-the-wild condition than machine corruption. However, considering its significance for LMM robustness, we have taken it into account for the first time. We sincerely hope that more future work will consider this dimension to improve the LMM’s resistance to distortion through carefully collected image pairs and further generalize its application in embodied intelligence.

#### A.5 FINANCIAL DISCLAIMER

Due to financial constraints, we can only try to be as comprehensive as possible in our academic content, such as the corruption dimension, and are not able to consider all cameras and robots on the market. This may lead to unavoidable limitations in the content. At the same time, since we do not have access to some of the LMM’s temperature parameters, the overly arbitrary play of the output may lead to its unsatisfactory R-Bench ranking. The R-Bench here is only an academic inquiry, not directed at any LMM developer, and does not involve any economic-related rankings. Anyone is welcome to retest their model against R-Bench if needed. We will be happy to update it on the list.

## REFERENCES

- Marah Abdin, Sam Ade Jacobs, Ammar Ahmad Awan, Jyoti Aneja, Ahmed Awadallah, Hany Awadalla, Nguyen Bach, Amit Bahree, Arash Bakhtiari, Harkirat Behl, et al. Phi-3 technical report: A highly capable language model locally on your phone. *arXiv preprint arXiv:2404.14219*, 2024.
- Josh Achiam, Steven Adler, Sandhini Agarwal, Lama Ahmad, Ilge Akkaya, Florencia Leoni Aleman, Diogo Almeida, Janko Altenschmidt, Sam Altman, Shyamal Anadkat, et al. Gpt-4 technical report. *arXiv preprint arXiv:2303.08774*, 2023.
- Peter Anderson, Basura Fernando, Mark Johnson, and Stephen Gould. Spice: Semantic propositional image caption evaluation. In *Computer Vision–ECCV 2016: 14th European Conference, Amsterdam, The Netherlands, October 11–14, 2016, Proceedings, Part V 14*, pp. 382–398. Springer, 2016.
- Guangji Bai, Zheng Chai, Chen Ling, Shiyu Wang, Jiaying Lu, Nan Zhang, Tingwei Shi, Ziyang Yu, Mengdan Zhu, Yifei Zhang, et al. Beyond efficiency: A systematic survey of resource-efficient large language models. *arXiv preprint arXiv:2401.00625*, 2024.
- Jinze Bai, Shuai Bai, Shusheng Yang, Shijie Wang, Sinan Tan, Peng Wang, Junyang Lin, Chang Zhou, and Jingren Zhou. Qwen-vl: A frontier large vision-language model with versatile abilities. *arXiv preprint arXiv:2308.12966*, 2023.
- Chaofeng Chen, Jiadi Mo, Jingwen Hou, Haoning Wu, Liang Liao, Wenxiu Sun, Qiong Yan, and Weisi Lin. Topiq: A top-down approach from semantics to distortions for image quality assessment. *IEEE Transactions on Image Processing*, 33:2404–2418, 2024a. doi: 10.1109/TIP.2024.3378466.
- Lin Chen, Jisong Li, Xiaoyi Dong, Pan Zhang, Conghui He, Jiaqi Wang, Feng Zhao, and Dahua Lin. Sharegpt4v: Improving large multi-modal models with better captions. *arXiv preprint arXiv:2311.12793*, 2023.
- Zhe Chen, Jiannan Wu, Wenhui Wang, Weijie Su, Guo Chen, Sen Xing, Muyan Zhong, Qinglong Zhang, Xizhou Zhu, Lewei Lu, Bin Li, Ping Luo, Tong Lu, Yu Qiao, and Jifeng Dai. Internvl: Scaling up vision foundation models and aligning for generic visual-linguistic tasks. In *Proceedings of the IEEE/CVF Conference on Computer Vision and Pattern Recognition (CVPR)*, pp. 24185–24198, June 2024b.
- Cisco. Cisco Visual Networking Index: Forecast and Trends, 2018–2023. *White Paper*, 2020.
- Francesco Croce, Maksym Andriushchenko, Vikash Sehwag, Edoardo Debenedetti, Nicolas Flammarion, Mung Chiang, Prateek Mittal, and Matthias Hein. Robustbench: a standardized adversarial robustness benchmark. In J. Vanschoren and S. Yeung (eds.), *Proceedings of the Neural Information Processing Systems Track on Datasets and Benchmarks*, volume 1, 2021.
- Xuanming Cui, Alejandro Aparcero, Young Kyun Jang, and Ser-Nam Lim. On the robustness of large multimodal models against image adversarial attacks. In *Proceedings of the IEEE/CVF Conference on Computer Vision and Pattern Recognition (CVPR)*, pp. 24625–24634, June 2024.
- Wenliang Dai, Junnan Li, Dongxu Li, Anthony Meng Huat Tiong, Junqi Zhao, Weisheng Wang, Boyang Li, Pascale Fung, and Steven Hoi. Instructblip: Towards general-purpose vision-language models with instruction tuning, 2023.
- Xiaoyi Dong, Pan Zhang, Yuhang Zang, Yuhang Cao, Bin Wang, Linke Ouyang, Xilin Wei, Songyang Zhang, Haodong Duan, Maosong Cao, Wenwei Zhang, Yining Li, Hang Yan, Yang Gao, Xinyue Zhang, Wei Li, Jingwen Li, Kai Chen, Conghui He, Xingcheng Zhang, Yu Qiao, Dahua Lin, and Jiaqi Wang. Internlm-xcomposer2: Mastering free-form text-image composition and comprehension in vision-language large model. *arXiv preprint arXiv:2401.16420*, 2024.
- Zhengxiao Du, Yujie Qian, Xiao Liu, Ming Ding, Jiezhong Qiu, Zhilin Yang, and Jie Tang. Glm: General language model pretraining with autoregressive blank infilling. In *Proceedings of the 60th Annual Meeting of the Association for Computational Linguistics (Volume 1: Long Papers)*, pp. 320–335, 2022.

- Vlad Hosu, Franz Hahn, Mohsen Jenadeleh, Hanhe Lin, Hui Men, Tamás Szirányi, Shujun Li, and Dietmar Saupe. The konstanz natural video database (konvid-1k). In *2017 Ninth international conference on quality of multimedia experience*, pp. 1–6. IEEE, 2017.
- Bo Li, Yuanhan Zhang, Dong Guo, Renrui Zhang, Feng Li, Hao Zhang, Kaichen Zhang, Yanwei Li, Ziwei Liu, and Chunyuan Li. Llava-onevision: Easy visual task transfer. *arXiv preprint arXiv:2408.03326*, 2024a.
- Chunyi Li, Zicheng Zhang, Wei Sun, Xiongkuo Min, and Guangtao Zhai. A full-reference quality assessment metric for cartoon images. In *IEEE 24th International Workshop on Multimedia Signal Processing*, 2022.
- Chunyi Li, Zicheng Zhang, Haoning Wu, Wei Sun, Xiongkuo Min, Xiaohong Liu, Guangtao Zhai, and Weisi Lin. Agiqa-3k: An open database for ai-generated image quality assessment. *IEEE Transactions on Circuits and Systems for Video Technology*, 2023.
- Chunyi Li, Haoning Wu, Hongkun Hao, Zicheng Zhang, Tengchaun Kou, Chaofeng Chen, Lei Bai, Xiaohong Liu, Weisi Lin, and Guangtao Zhai. G-refine: A general quality refiner for text-to-image generation. *arXiv preprint arXiv:2404.18343*, 2024b.
- Chunyi Li, Haoning Wu, Zicheng Zhang, Hongkun Hao, Kaiwei Zhang, Lei Bai, Xiaohong Liu, Xiongkuo Min, Weisi Lin, and Guangtao Zhai. Q-refine: A perceptual quality refiner for ai-generated image. *arXiv preprint arXiv:2401.01117*, 2024c.
- Chunyi Li, Xiele Wu, Haoning Wu, Donghui Feng, Zicheng Zhang, Guo Lu, Xiongkuo Min, Xiaohong Liu, Guangtao Zhai, and Weisi Lin. Cmc-bench: Towards a new paradigm of visual signal compression. *arXiv preprint arXiv:2406.09356*, 2024d.
- Feng Li, Renrui Zhang, Hao Zhang, Yuanhan Zhang, Bo Li, Wei Li, Zejun Ma, and Chunyuan Li. Llava-next-interleave: Tackling multi-image, video, and 3d in large multimodal models. *arXiv preprint arXiv:2407.07895*, 2024e.
- Zhang Li, Biao Yang, Qiang Liu, Zhiyin Ma, Shuo Zhang, Jingxu Yang, Yabo Sun, Yuliang Liu, and Xiang Bai. Monkey: Image resolution and text label are important things for large multi-modal models. In *proceedings of the IEEE/CVF conference on computer vision and pattern recognition*, 2024f.
- Hanhe Lin, Vlad Hosu, and Dietmar Saupe. Kadid-10k: A large-scale artificially distorted iqa database. In *2019 Tenth International Conference on Quality of Multimedia Experience (QoMEX)*, pp. 1–3. IEEE, 2019.
- Tsung-Yi Lin, Michael Maire, Serge Belongie, James Hays, Pietro Perona, Deva Ramanan, Piotr Dollár, and C Lawrence Zitnick. Microsoft coco: Common objects in context. In *Computer Vision–ECCV 2014: 13th European Conference, Zurich, Switzerland, September 6–12, 2014, Proceedings, Part V 13*, pp. 740–755. Springer, 2014.
- Haotian Liu, Chunyuan Li, Yuheng Li, and Yong Jae Lee. Improved baselines with visual instruction tuning. *arXiv:2310.03744*, 2023a.
- Haotian Liu, Chunyuan Li, Qingyang Wu, and Yong Jae Lee. Visual instruction tuning. In A. Oh, T. Naumann, A. Globerson, K. Saenko, M. Hardt, and S. Levine (eds.), *Advances in Neural Information Processing Systems*, volume 36, pp. 34892–34916. Curran Associates, Inc., 2023b.
- Yuan Liu, Haodong Duan, Yuanhan Zhang, Bo Li, Songyang Zhang, Wangbo Zhao, Yike Yuan, Jiaqi Wang, Conghui He, Ziwei Liu, et al. Mmbench: Is your multi-modal model an all-around player? *arXiv preprint arXiv:2307.06281*, 2023c.
- Haoyu Lu, Wen Liu, Bo Zhang, Bingxuan Wang, Kai Dong, Bo Liu, Jingxiang Sun, Tongzheng Ren, Zhusuo Li, Yaofeng Sun, et al. Deepseek-vl: towards real-world vision-language understanding. *arXiv preprint arXiv:2403.05525*, 2024.
- Kenneth Marino, Mohammad Rastegari, Ali Farhadi, and Roozbeh Mottaghi. Ok-vqa: A visual question answering benchmark requiring external knowledge. In *Proceedings of the IEEE/cvf conference on computer vision and pattern recognition*, pp. 3195–3204, 2019.

- Kishore Papineni, Salim Roukos, Todd Ward, and Wei-Jing Zhu. Bleu: a method for automatic evaluation of machine translation. In *Proceedings of the 40th annual meeting of the Association for Computational Linguistics*, pp. 311–318, 2002.
- Jielin Qiu, Yi Zhu, Xingjian Shi, F. Wenzel, Zhiqiang Tang, Ding Zhao, Bo Li, and Mu Li. Benchmarking robustness of multimodal image-text models under distribution shift. *Journal of Data-centric Machine Learning Research (DMLR)*, 2024.
- Madeline C Schiappa, Shruti Vyas, Hamid Palangi, Yogesh S Rawat, and Vibhav Vineet. Robustness analysis of video-language models against visual and language perturbations. In *Proceedings of the 36th International Conference on Neural Information Processing Systems*, pp. 34405–34420, 2022.
- Christian Schlarmann and Matthias Hein. On the adversarial robustness of multi-modal foundation models. In *Proceedings of the IEEE/CVF International Conference on Computer Vision (ICCV) Workshops*, pp. 3677–3685, October 2023.
- Gemini Team. Gemini 1.5: Unlocking multimodal understanding across millions of tokens of context. *arXiv preprint arXiv:2403.05530*, 2024.
- Ramakrishna Vedantam, C Lawrence Zitnick, and Devi Parikh. Cider: Consensus-based image description evaluation. In *Proceedings of the IEEE conference on computer vision and pattern recognition*, pp. 4566–4575, 2015.
- Peng Wang, Shuai Bai, Sinan Tan, Shijie Wang, Zhihao Fan, Jinze Bai, Keqin Chen, Xuejing Liu, Jialin Wang, Wenbin Ge, et al. Qwen2-vl: Enhancing vision-language model’s perception of the world at any resolution. *arXiv preprint arXiv:2409.12191*, 2024.
- Jason Wei, Yi Tay, Rishi Bommasani, Colin Raffel, Barret Zoph, Sebastian Borgeaud, Dani Yogatama, Maarten Bosma, Denny Zhou, Donald Metzler, et al. Emergent abilities of large language models. *arXiv preprint arXiv:2206.07682*, 2022.
- Haoning Wu, Zicheng Zhang, Erli Zhang, Chaofeng Chen, Liang Liao, Annan Wang, Chunyi Li, Wenxiu Sun, Qiong Yan, Guangtao Zhai, et al. Q-bench: A benchmark for general-purpose foundation models on low-level vision. *arXiv preprint arXiv:2309.14181*, 2023a.
- Haoning Wu, Zicheng Zhang, Weixia Zhang, Chaofeng Chen, Liang Liao, Chunyi Li, Yixuan Gao, Annan Wang, Erli Zhang, Wenxiu Sun, et al. Q-align: Teaching lmms for visual scoring via discrete text-defined levels. *arXiv preprint arXiv:2312.17090*, 2023b.
- XAI. grok-1.5v, 2024. URL <https://x.ai/blog/grok-1.5v>.
- Yuan Yao, Tianyu Yu, Ao Zhang, Chongyi Wang, Junbo Cui, Hongji Zhu, Tianchi Cai, Haoyu Li, Weilin Zhao, Zihui He, et al. Minicpm-v: A gpt-4v level mllm on your phone. *arXiv preprint arXiv:2408.01800*, 2024.
- Jiabo Ye, Haiyang Xu, Haowei Liu, Anwen Hu, Ming Yan, Qi Qian, Ji Zhang, Fei Huang, and Jingren Zhou. mplug-owl3: Towards long image-sequence understanding in multi-modal large language models. *arXiv preprint arXiv:2408.04840*, 2024a.
- Qinghao Ye, Haiyang Xu, Jiabo Ye, Ming Yan, Anwen Hu, Haowei Liu, Qi Qian, Ji Zhang, and Fei Huang. mplug-owl2: Revolutionizing multi-modal large language model with modality collaboration. In *Proceedings of the IEEE/CVF Conference on Computer Vision and Pattern Recognition*, pp. 13040–13051, 2024b.
- Weihao Yu, Zhengyuan Yang, Linjie Li, Jianfeng Wang, Kevin Lin, Zicheng Liu, Xinchao Wang, and Lijuan Wang. Mm-vet: Evaluating large multimodal models for integrated capabilities. In *Forty-first International Conference on Machine Learning*, 2024.
- Jiawei Zhang, Tianyu Pang, Chao Du, Yi Ren, Bo Li, and Min Lin. Benchmarking large multimodal models against common corruptions. *arXiv preprint arXiv:2401.11943*, 2024a.

Weixia Zhang, Guangtao Zhai, Ying Wei, Xiaokang Yang, and Kede Ma. Blind image quality assessment via vision-language correspondence: A multitask learning perspective. In *Proceedings of the IEEE/CVF Conference on Computer Vision and Pattern Recognition*, pp. 14071–14081, 2023.

Yi-Jun Zhang, Zhao-Fei Yu, Jian K Liu, and Tie-Jun Huang. Neural decoding of visual information across different neural recording modalities and approaches. *Machine Intelligence Research*, 19(5):350–365, 2022.

Zicheng Zhang, Haoning Wu, Chunyi Li, Yingjie Zhou, Wei Sun, Xiongkuo Min, Zijian Chen, Xiaohong Liu, Weisi Lin, and Guangtao Zhai. A-bench: Are Imms masters at evaluating ai-generated images? *arXiv preprint arXiv:2406.03070*, 2024b.

Yunqing Zhao, Tianyu Pang, Chao Du, Xiao Yang, Chongxuan Li, Ngai-Man Cheung, and Min Lin. On evaluating adversarial robustness of large vision-language models. In *Thirty-seventh Conference on Neural Information Processing Systems*, 2023.